Article published online: 2022-09-19

Novel Docetaxel-Loaded Micelles Based on all-*trans*-Retinoic Acid: Preparation and Pharmacokinetic Study in Rats

Ya-Ni Yang[1,#] Jia-Jia Cheng[1,#] Jun He[1*] Wei-Gen Lu[1*]

[1] National Pharmaceutical Engineering Research Center, China State Institute of Pharmaceutical Industry, Shanghai, People's Republic of China

Pharmaceut Fronts 2022;4:e188–e196.

Address for correspondence Jun He, PhD, National Pharmaceutical Engineering Research Center, China State Institute of Pharmaceutical Industry, 285 Gebaini Road, Shanghai 201203, People's Republic of China (e-mail: chinaynhe@163.com).

Wei-Gen Lu, PhD, National Pharmaceutical Engineering Research Center, China State Institute of Pharmaceutical Industry, 285 Gebaini Road, Shanghai 201203, People's Republic of China (e-mail: sipiluwg@163.com).

Abstract

Docetaxel (DTX) is a poorly soluble drug. The purpose of this study was to explore a DTX-loaded micelle delivery system using *N*-(all-*trans*-retinoyl)-*L*-cysteic acid methyl ester sodium salt (XMeNa) as the carrier materials. In this study, amphiphilic surfactant XMeNa was synthesized. Then, the blood biocompatibility and the value of critical micelle concentration (CMC) were assessed by a hemolysis test and pyrene-based fluorescent probe techniques, respectively. The XM-DTX micelles were prepared using the method of thin-film hydration, and characterized by dynamic light scattering and transmission electron microscopy (TEM). The entrapment efficiency (EE) and drug loading efficiency (DLE) were assessed by the ultrafiltration method. *In vitro* release and pharmacokinetic behaviors of XM-DTX micelles were performed in rats using Taxotere (a commercialized DTX injection) as a control. Our data confirmed the excellent blood biocompatibility of XMeNa as a carrier. XMeNa can self-assemble into micelles in aqueous media with a very low CMC (6.2 μg/mL). The average size and zeta potential of the XM-DTX micelles were 17.3 ± 0.2 nm, and -41.6 ± 0.3 mV, respectively. EE and DLE reached up to $95.3 \pm 0.7\%$ and $22.4 \pm 0.2\%$, respectively, which may account for the high solubility of DTX in normal saline. The micelles were spherical in TEM with good dispersion and no aggregation and adhesion, and exhibited good stability after reconstitution over 8 hours. Results from *in vitro* release assay suggested a much slower release behavior of XM-DTX micelles in comparison to Taxotere. Additionally, XM-DTX micelles prolonged DTX retention in blood circulation, increased the area under the curve by 2.4-fold, and significantly decreased the clearance of the drug. Given above, the XM-DTX micelles could improve the solubility and the release of DTX. The amphiphilic surfactant XMeNa also exhibited great potential as a vehicle for exploring delivery of poorly water soluble drugs in the future.

Keywords

- micelles
- docetaxel
- all-*trans*-retinoic acid
- pharmacokinetic
- surfactant

[#] *These authors contributed equally to this work.*

received
April 17, 2022
accepted
June 16, 2022

DOI https://doi.org/10.1055/s-0042-1757511.
ISSN 2628-5088.

Georg Thieme Verlag KG, Rüdigerstraße 14, 70469 Stuttgart, Germany

Introduction

Docetaxel (DTX), a typical taxane, has been approved as a first-line antitumor drug in clinical treatments, including breast cancer, nonsmall cell lung cancer, and castration-resistant prostate cancer.[1–4] It can effectively inhibit the proliferation of rapidly growing cells by stabilizing the microtubule during mitosis.[5] However, its poor water solubility prevents the full exploitation of the drug. Taxotere is the current marked formulation of the DTX, yet, used polysorbate 80 and ethanol as the co-solvent that might induce adverse reactions following intravenous injection.[6,7] Thus, developing a novel DTX delivery system with improved solubility is of important significance.

Notably, nanotechnology has played an important role in improving the properties of DTX for appropriate application.[8,9] Over the past decades, nanoparticles and micelles have been widely developed as DTX delivery systems to conceal the weak solubility of the drug.[10–12] Micelles are self-assembled core-shell nanocarriers formed by surfactants or polymers. The micellar drug formulation can passively target solid tumors (even poorly permeable tumors) and effectively internalize cells due to its smaller particle size (10–100 nm).[13] Moreover, micelles have higher vascular permeability, and are not easily opsonized by plasma proteins, which enables them to effectively avoid phagocytosis by the reticuloendothelial system (RES) and reduce renal excretion, and thus the circulation time of micelles in blood is considerably long.[14] In addition to the advantages mentioned above, micelles have ease of production, have a high drug loading rate (up to 30%), and small particle sizes,[15] which make them a good choice for improving the safety and therapeutic efficacy of intravenous formulations.[16]

A nano-sized micellar formulation of paclitaxel (PTX; Apealea/Paclica) has been approved by European Medicines Agency (EMA) in 2018, in which isoforms of retinoic acid derivatives were used as micelle-forming excipients to enhance water solubility of the drug.[17] It has also received market authorization in Russia (2015) and Kazakhstan (2017). PTX is formulated with the surfactants that consist of an equimolar mixture of two *iso*-forms of *N*-retinoyl-*L*-cysteic acid methyl ester sodium salt (XR17). Once reconstituted in an aqueous solution for infusion, the drug and the surfactant are present as micelles at sizes of 20 to 30 nm in a clear solution. The Cremophor EL-free PTX micellar formulation allows a shorter infusion time and can be administered at a high dose without mandatory premedication, which possibly reduce excipient-induced systemic toxicity and hypersensitivity reactions.[18] A crossover study of the PTX micellar formulation and nab-PTX demonstrated that the two formulations met bioequivalence criteria, and supported safe administration of the PTX micellar formulation with no serious events or deaths reported.[19] Given the success of the PTX micellar formulation (Apealea), this study synthesized a surfactant, *N*-(all-*trans*-retinoyl)-*L*-cysteic acid methyl ester sodium salt (XMeNa), and then used it as a solubilizer to prepare a DTX-loaded micelle delivery system (XM-DTX) to improve the solubility and avoid side effects of the drug. The micelles were prepared and characterized in terms of particle size, drug loading, *in vitro* release, and pharmacokinetic behaviors in rats. Our data suggested that the all-*trans*-retinoic acid-based micelles may be an effective delivery system for poorly water-soluble drugs.

Materials and Methods

All-*trans*-retinoic acid was purchased from Nanjing Dulai Biotechnology Co., Ltd. (Jiangsu, China). All chemicals and reagents used in this study were of analytical grade and obtained from Sinopharm Chemical Reagent Co., Ltd. (Shanghai, China). DTX was procured from Chongqing Taihao Pharmaceutical Co., Ltd. (Chongqing, China). Taxotere (DTX injection) was obtained from Sanofi (Hangzhou) Pharmaceutical Co., Ltd. (Zhejiang, China).

Synthesis of XMeNa

An amphiphilic drug carrier of XMeNa was synthesized according to previous reports (►**Fig. 1**).[20,21] Based on retrosynthetic analysis, XMeNa was obtained in two steps.

The first objective was to synthesize *L*-cysteic acid methyl ester (LAME). Briefly, *L*-cysteic acid monohydrate (28 g, 0.15 mol) was suspended in methanol (700 mL), stirred for 5 to 10 minutes at room temperature (r.t.), and then thionyl chloride ($SOCl_2$, 80 mL, 1.07 mol) was added dropwise. The resulting solution was stirred for 10 hours, and the reaction was monitored by thin layer chromatography. After the reaction was completed, methanol was evaporated to give a crude product of LAME, which was washed by anhydrous ethanol–methyl *tert*-butyl ether (1:1, v/v), filtered, and then dried at 50°C under vacuum to obtain the target compounds as white powder.

Subsequently, XMeNa was prepared as follows. A mixture of all-*trans*-retinoic acid (9 mmol), tetrahydrofuran (THF)–acetonitrile (1:2, v/v), and triethylamine (TEA; 10 mmol) was stirred at −20°C. Butylchloroformate (9.9 mmol) was added slowly, and the mixture was stirred for 30 minutes. Then, LAME (13.5 mmol), *N*,*N*-dimethylformamide (60 mL), and TEA (2.4 mL) were added and the reaction mixture was stirred for 2.5 hours at 25°C before the removal of solvents. The residue was stirred with saturated aqueous sodium bicarbonate ($NaHCO_3$) and purified with methyl *tert*-butyl ether. The aqueous solution was saturated with sodium chloride, and added ethyl acetate for extraction. The combined organic layers were dried, filtered, and concentrated to give the target product.

XMeNa Characterization

Identification of LAME and XMeNa

Proton nuclear magnetic resonance (^{1}H NMR) spectra of LAME and XMeNa were recorded on a Bruker Ascend spectrometer operating at 400 MHz. Electrospray ionization mass-spectrometry (ESI-MS) was acquired with a Waters Micromass Q-TOF run in a liner mode.

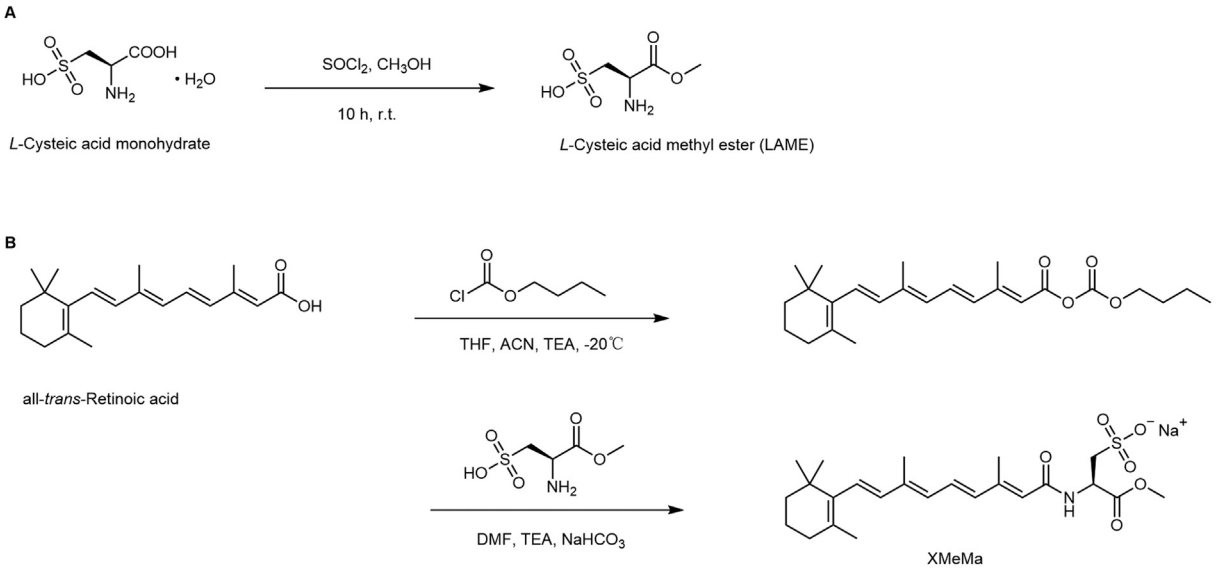

Fig. 1 Synthetic routes of (**A**) LAME and (**B**) XMeNa.

Stability study of XMeNa

The stability of XMeNa was examined in the solid form at r.t. under normal ambient light/dark for 10 days, and in methanol and ethanol over 180 days at 4°C, respectively. High-performance liquid chromatography (HPLC) analysis of XMeNa was performed on an Agilent 1260 HPLC System (Agilent, United States) under the following conditions: an Ultimate XB-C18 column (250 mm × 4.6 mm, 5 µm, Welch, Shanghai, China) was used with a mobile phase of acetonitrile/20 mmol/L potassium dihydrogen phosphate in water (55/45, v/v) at a flow rate of 1.2 mL/min. The UV detection wavelength was performed at 350 nm and the column temperature was set to 40°C. Each sample was dissolved in methanol (0.5 mg/mL), and 10 µL was injected for HPLC analysis. The content of XMeNa in the tested solution was calculated via the external standard method.

Critical Micelle Concentration Determination

The critical micelle concentration (CMC) was determined using pyrene-based fluorescent probe techniques according to a reported study.[22] Briefly, a pyrene solution in acetone (5×10^{-5} mol/L) was added dropwise to a brown volumetric flask. Next, the acetone was completely evaporated at r.t. XMeNa solutions at appropriate concentrations (0.00001 to 1 mg/mL in water) in the assay buffer were added to the vials to obtain a final concentration of 5×10^{-7} mol/L of pyrene. The obtained solutions were incubated at 37°C, at 50 rpm for 6 hours in the dark. The fluorescence intensity in each vial was then determined using a spectrofluorometer at an excitation wavelength of 334 nm and emission wavelengths of 375 nm for I_1 and 384 nm for I_3. The CMC was given as the concentration for which an intersection of two straight lines of the I_3/I_1 ratio was observed.

Hemolysis Assay

Red blood cells (RBCs) from rats were extracted (removing white bold cells and platelets) and suspended in normal saline containing 2% (v/v) RBCs. XMeNa solutions (0.5 mL) were tested for hemolysis at a concentration range of 0.01 to 2 mg/mL, using 2% RBCs solution (2.5 mL), in a solution made up to 5 mL using normal saline. A positive control consisting of RBCs using distilled water and a negative control consisting of RBCs incubated in normal saline were also prepared. These XMeNa–RBCs solutions and controls (10 tubes in total) were incubated at 37°C for 2 hours, followed by centrifugation at 500 *g* for 5 minutes. Absorbance of the supernatants was measured at 570 nm using a spectrophotometer and the percent hemolysis was calculated for each supernatant and plotted against XMeNa concentrations. The percent hemolysis was calculated using Eqn. (1):

$$\text{Hemolysis (\%)} = \frac{\text{Sample absorbance} - \text{Negative control absorbance}}{\text{Positive control absorbance} - \text{Negative control absorbance}} \times 100\% \quad (1)$$

Preparation of the XM-DTX Micelles

XM-DTX micelles were prepared by a thin-film hydration technique with a 2.5:1 (w/w) ratio of XMeNa to DTX (►**Fig. 2**). XMeNa (50 mg) and DTX (20 mg) were dissolved in 3 mL methanol and the solvent was removed via evaporation under vacuum at 40°C to form a stripped film. The resulting thin film was hydrated with 2 mL of deionized water at 40°C. Nonencapsulated DTX was removed by filtration of the micelle suspensions through a 0.22 µm microporous membrane filter. The solution was lyophilized with a freezer dryer (VirTis Advantage, SP Scientific) using a designed procedure. The micellar preparations were stored at 4°C for further experiments.

Characterization of XM-DTX Micelles

Particle Size, Zeta Potential, Morphological and Stability Analysis

Particle size, polydispersity index (PDI), and zeta potential of the XM-DTX micelles were determined via dynamic light scattering (DLS; Malvern Zetasizer Nano ZS, United

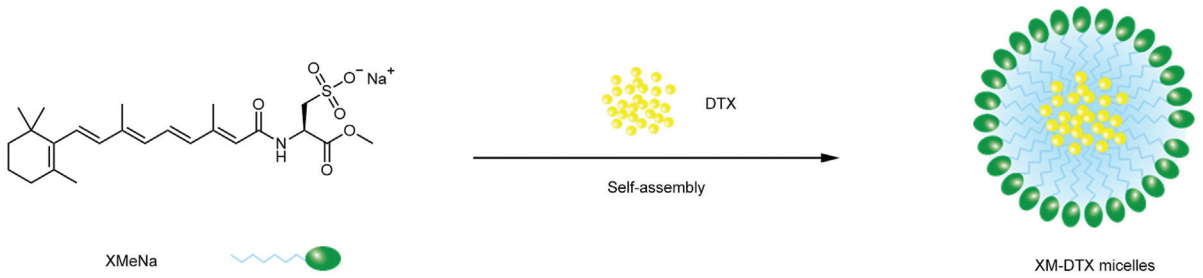

Fig. 2 Schematic illustration of preparation of XM-DTX micelles.

Kingdom) with a scattering angle of 90° at 25°C after reconstituting the micelles to an appropriate volume with normal saline.

Transmission electron microscopy (TEM; JEM-2011, JEOL, Japan) was used to visualize the morphological features of the prepared micelles. The sample was allowed to dry on a 400 mesh copper grid with carbon film coating. The image was obtained with 200 kV voltage.

After reconstitution, the stability of XM-DTX micelles over 24 hours was further determined by monitoring the particle size distribution using DLS.

Determination of the Entrapment Efficiency and Drug Loading Efficiency

To determine the entrapment efficiency (EE) and drug loading efficiency (DLE) of XM-DTX micelles, 10 mg of the freeze-dried powder was reconstituted in 10 mL normal saline. Ultrafiltration centrifugation (7,500 *g*, 20 minutes) was then used to remove the unentrapped drugs. The content of encapsulated DTX was evaluated on a Shimadzu LC-20AD series HPLC system equipped with a SPD-20A UV detector and a CTO-20A thermostatic column compartment (Shimadzu, Japan). The mobile phase consisting of acetonitrile and water (55:45, v/v) was pumped through a C18 column (250 mm × 4.6 mm, 5 µm, Dikma, China) at a flow rate of 1.0 mL/min and the eluent was monitored at 229 nm. The injected sample volume was 20 µL. The standard curve of DTX was prepared using acetonitrile DTX with the concentrations ranging from 20 to 500 µg/mL, with coefficients of determination (r^2) above 0.999. The limit of quantification (LOQ) was 0.05 µg/mL, determined at a signal-to-noise ratio of 10. The EE and DLE values were calculated using Eqn. (2) and (3), respectively:

$$\mathrm{EE} = \frac{\text{Weight of encapsulated DTX in micelles}}{\text{Total weight of DTX}} \times 100\% \quad (2)$$

$$\mathrm{DLE} = \frac{\text{Weight of encapulated DTX in micelles}}{\text{Weight of final formulation}} \times 100\% \quad (3)$$

In Vitro DTX Release Profile

The *in vitro* release of DTX from the micelles was investigated using a dialysis method. Phosphate-buffered saline (PBS; pH 7.4) containing 0.1% Tween 80 was selected as the release medium. Briefly, appropriate lyophilized power of XM-DTX micelles equivalent to 1 mg of DTX was dispersed to 1 mL of the release medium, and added into a dialysis bag (8,000–14,000 Da). Then, the sealed bag was placed into a container with 100 mL release medium, which was kept at 37 ± 0.5°C with continuous shaking in an incubator shaker at 100 rpm. At predetermined time intervals, samples (2 mL) of release solution were removed and immediately replaced with the same volume of fresh release medium ($n = 3$). A parallel dialysis, in which a dialysis bag containing the same amount of DTX in Taxotere (treated with DTX commercial solution of 10 mg/mL and diluted to 1 mg/mL with the release medium), was used for comparison. The concentration of DTX in the release medium was determined using the HPLC method as described above.

Pharmacokinetics

Sprague-Dawley (SD) rats (male, weighed 200–220 g) were purchased from Shanghai Laboratory Animal Center (Shanghai, China). The animals were housed in standard cages and under light conditions, fed a standard diet, and had free access to water. The animals were fasted for 12 hours prior to drug administration but given free access to water. The use of rats in the experiment was approved by the Ethics Committee of Fudan University, and animal handling was performed in accordance with the Guidelines on Laboratory Animal Welfare issued by the Ministry of Science and Technology of the People's Republic of China.

Male SD rats were randomized into XM-DTX and Taxotere groups ($n = 6$ in each group). Rats in the XM-DTX group were intravenously (iv) administered with XM-DTX micelles (DTX dose of 10 mg/kg) via the tail vein, and rats in the Taxotere group were administered in the same way as the XM-DTX group, except that DTX commercial solution with a dose of 10 mg/kg was given. Then, blood was withdrawn through retro-orbital bleeding by heparinized capillary tubes at 0.083, 0.25, 0.5, 1, 2, 4, 6, 8, 10, and 24 hours. The collected blood was mixed with heparin sodium and immediately centrifuged (12,000 *g*, 3 minutes at 4°C). Plasma samples (100 µL) were transferred into centrifuge tubes, mixed with 100 µL of PTX acetonitrile solution (PTX as the internal standard substance, 5 µg/mL) and 200 µL of acetonitrile, vortexed for 3 minutes, and then centrifuged at 4°C for 3 minutes at 12,000 *g*. The supernatant was collected. The DTX content was measured using HPLC as described in the Determination of the Entrapment Efficiency and Drug Loading Efficiency section. In parallel, the drug and PTX were spiked into the plasma, and a standard DTX calibration curve was obtained with the concentrations of DTX in the range of

0.05 (LOQ) to 10 μg/mL as the abscissa, and the peak area ratio of DTX to PTX as the ordinate, with r^2 above 0.997. The content of DTX was calculated according to the calibration curves with the internal standard method.

Statistical Analysis

The results were depicted as average ± standard deviation. Statistical analyses of data were performed using one-way analysis of variance (ANOVA), and Tukey's significant difference was used post hoc to compare differences between individual groups. A p-value <0.05 was accepted as statistically significant.

Results and Discussions

Synthesis and Characterization of XMeNa

Identification of the Synthesized Compound: ^{1}H NMR and ESI-MS

LAME was synthesized using the above method with an 85% yield. As shown in ►**Fig. 3A**, ^{1}H NMR (400 MHz, D_2O) δ 4.53 (dd, $J = 7.0$, 4.1 Hz, 1H), 3.82 (s, 3H), 3.48 (qd, $J = 15.1$, 5.6 Hz, 2H). MS (ESI+, m/z) $[M+H]^+$: 184.04, $[M-H]^-$: 182.07. These results implied the successful synthesis of LAME.

XMeNa was obtained with a 90% yield and 99.79% purity. As shown in ►**Fig. 3B**, ^{1}H NMR (400 MHz, CD_3OD) δ 8.00 (s, 1H), 7.75 (d, $J = 15.4$ Hz, 1H), 7.00 (dd, $J = 15.4$, 11.4 Hz, 1H), 6.22 (dt, $J = 26.3$, 16.1 Hz, 3H), 5.78 (s, 1H), 4.83 (dd, $J = 6.7$, 4.8 Hz, 1H), 3.77 (s, 3H), 2.95 (d, $J = 53.2$ Hz, 2H), 2.08 (d, $J = 1.0$ Hz, 3H), 2.05 (d, $J = 6.2$ Hz, 2H), 2.00 (d, $J = 11.1$ Hz, 3H), 1.73 (s, 3H), 1.66 (ddd, $J = 8.9$, 7.9, 4.5 Hz, 2H), 1.55 – 1.47 (m, 2H), 1.05 (s, 6H). ESI-MS was used to confirm the molecular weight of XMeNa, and revealed: m/z $[M-H]^-$: 464.44. These results were in good agreement with the previous report.[20] Based on these results, we conclude that XMeNa was successfully synthesized.

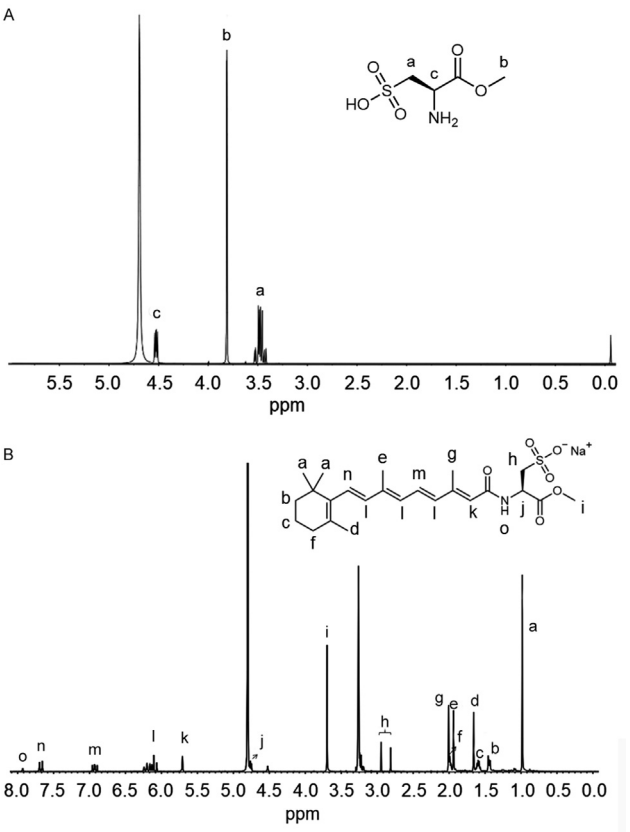

Fig. 3 ^{1}H NMR spectra of (**A**) LAME and (**B**) XMeNa.

Chemical Stability of XMeNa

The storage stability of XMeNa was studied in their solid form and in solution (methanol and ethanol). ►**Fig. 4A** shows that XMeNa solid, protected from light, was more stable at ambient temperature than under ambient light conditions. Such results were probably due to the unstable retinol part of all-*trans*-retinoic acid, which is responsible for the rapid degradation of the drug.[23] As shown in ►**Fig. 4B**, XMeNa was stable both in methanol and ethanol at 4°C for over 180 days, and less than 2% degradation was detected in methanol. Hence, our data suggested that XMeNa should be stored in methanol solution at 4°C and protected from light to avoid degradation, which were consistent with the published report.[17]

Determination of the CMC

As known, amphiphilic surfactants in aqueous solution could self-assemble into micelles at concentrations above their CMC. Micelles with low CMCs, an indication of micelles' stability, are necessary for intravenous applications.[24] The lower the CMC, the greater the stability of micelles. The

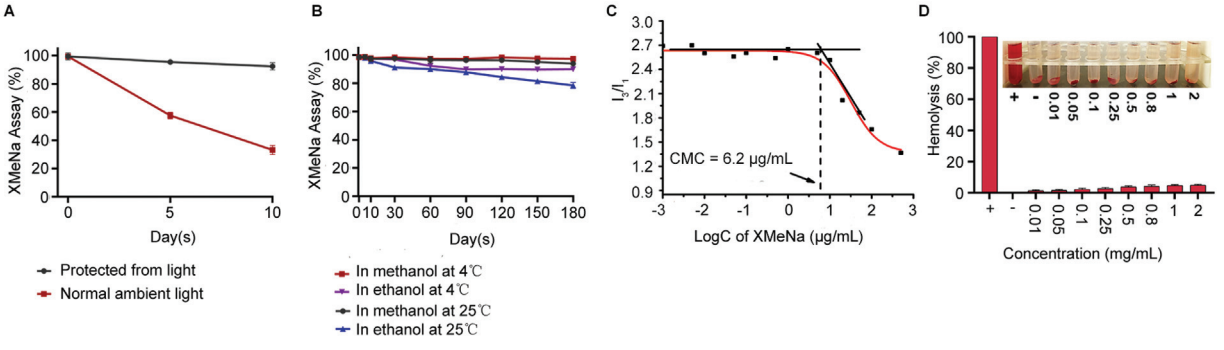

Fig. 4 Characterization of XMeNa. Chemical stability of XMeNa in (**A**) solid and in (**B**) methanol/ethanol. (**C**) The CMC value of XMeNa, assessed by pyrene-based fluorescent probe techniques. (**D**) Hemolysis test of different concentrations of XMeNa. CMC, critical micelle concentration.

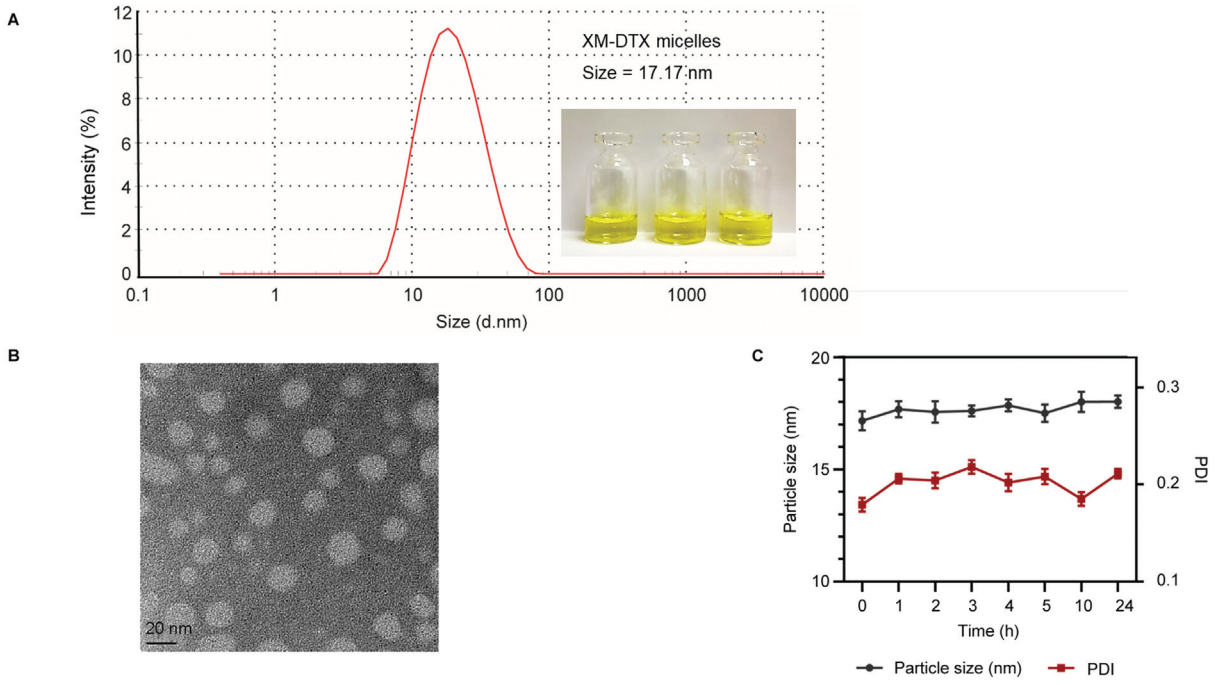

Fig. 5 Characterization and the stability assay of XM-DTX micelles. (**A**) Particle size profile and (**B**) TEM image (scale bar: 20 nm) of XM-DTX micelles. (**C**) Stability of the XM-DTX micelles after reconstitution assayed by the size and PDI over 24 hours. PDI, polydispersity index; TEM, transmission electron microscope.

pyrene method is one of the most sensitive methods for the determination of CMC values. ►**Fig. 4C** shows that the CMC of XMeNa was 6.2 µg/mL, determined by a fluorescence spectrophotometer using pyrene as a fluorescence probe. This assay monitors a change in fluorescence characteristics of pyrene that occurs when it is encapsulated in the micellar medium. In brief, the peak excitation of pyrene shifts from 334 nm (in polar environments) to 337 nm (in nonpolar environments). The CMC of XMeNa is significantly lower than those of conventional surfactants, such as sodium dodecyl sulfate (CMC = 2.39 mg/mL).[24] The lower CMC indicated that the micelles formed by XMeNa might exhibit a relatively high stability in systemic circulation upon dilution in the blood stream after iv injection.

Hemolysis Assay

An *in vitro* hemolysis test was conducted to assess the blood biocompatibility of XMeNa, which is an important factor in the development of new agents delivered intravenously. As shown in ►**Fig. 4D**, the hemolysis rates of XMeNa at different concentrations were far below the threshold value of 5%, indicating that XMeNa has excellent blood biocompatibility and is suitable for further intravenous study. More broadly, consideration of carrier's toxicity is critical to ensure that they have high biocompatibility. According to an EMA assessment report of Apealea, XR17 did not show cytotoxic effects up to 200 µg/mL, the maximum concentration tested,[17] which provides a fourfold safety margin based on a phase I randomized placebo-controlled study to assess the pharmacokinetics, safety, and tolerability in healthy subjects. Therefore, XMeNa is a suitable carrier of drug delivery for further clinical development.

Characterization of XM-DTX Micelles

Particle Size, Zeta Potential, Morphological, EE, DLE, and Stability Analyses

Physicochemical properties of micelles play a significant role in determining their fate after administration. The prepared DTX-loaded XM-DTX micelles were therefore characterized by particle size, zeta potential, morphology, EE, and LDE. As shown in ►**Fig. 5A**, the nanoscale sizes of XM-DTX micelles were 17.3 ± 0.2 nm, suggesting that the micelles were suitable for passive tumor targeting by enhancing permeation and retention effects, while reducing RES-mediated clearance (CL) and avoiding renal filtration.[25] Additionally, the micelles exhibited a negative zeta potential of −41.6 ± 0.3 mV, which was helpful for decreasing protein adsorption on the micelle surface, and might avoid CL by a mononuclear phagocyte system and led to a longer circulation lifetime.[26,27] Results from the TEM image provided a direct evidence that the XM-DTX micelles were uniformly spherical, well dispersed without aggregation and adhesion, and the average size was approximately 20 nm (►**Fig. 5B**). Moreover, the EE and DLE values of the prepared XM-DTX micelles were determined to be 95.3 ± 0.7% and 22.4 ± 0.2%, respectively, suggesting that DTX could be efficiently entrapped into the XM-DTX micelles.

Storing XM-DTX micelles in a powder form could alleviate potential pitfalls associated with storage in the solution form. Thus, we monitored the particle size of the micelles to evaluate whether the colloidal stability of the micelles was preserved after reconstitution. As shown in ►**Fig. 5C**, average particle sizes are stable at approximately 20 nm within 24 hours after the reconstitution of the lyophilized powders

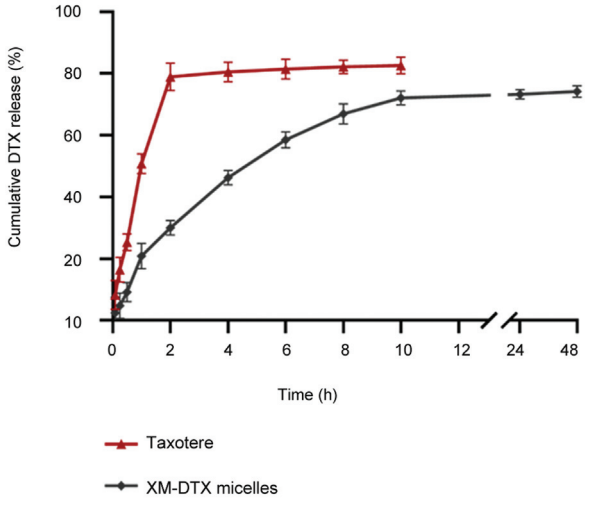

Fig. 6 Release pattern of DTX from Taxotere and XM-DTX micelles in phosphate buffer (pH = 7.4, release media contained 0.1% Tween 80) at 37°C. All results were displayed as mean ± SD ($n = 3$). DTX, docetaxel; SD, standard deviation.

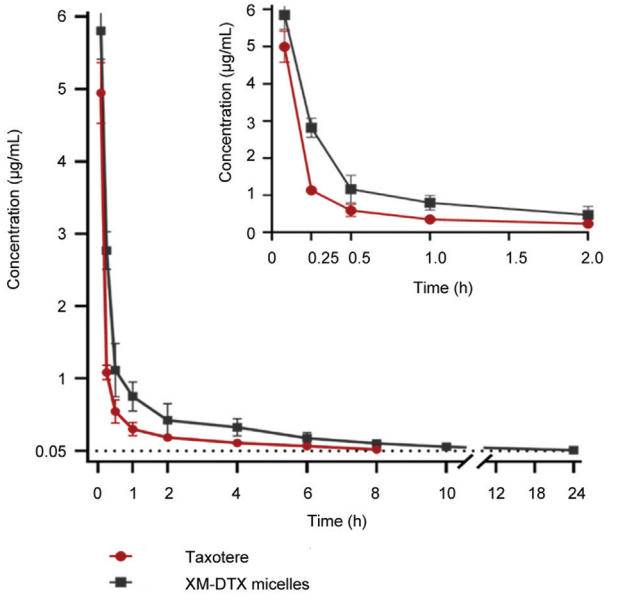

Fig. 7 Plasma concentration–time profiles of DTX in rats following intravenous administration of XM-DTX and Taxotere (10 mg/kg) (mean ± SD, $n = 6$). DTX, docetaxel; SD, standard deviation.

with normal saline. No significant changes were observed for the particle size and size distribution, indicating their superior colloidal stability.

In Vitro DTX Release Profile

The *in vitro* release behavior of DTX from XM-DTX micelles was investigated in PBS buffer (pH 7.4) containing 0.1% Tween 80 at 37°C. ►**Fig. 6** shows that 80.5 ± 3.2% of DTX from Taxotere diffused out of the dialysis bag at 4 hours; however, only 46.3 ± 2.4% of DTX was released from XM-DTX micelles at this time point. Inspiringly, only 74.2 ± 1.9% of DTX was released from the micelles at 48 hours. Our data suggested that XM-DTX micelles exhibited a comparable slower release profile in comparison to Taxotere. To achieve a better understanding of the mechanism of DTX release kinetics from XM-DTX micelles, each of the drug release stages was fitted with various mathematical models, including zero-order kinetics, first-order kinetics, the Higuchi model, and the Hixson–Crowell model.[28–30] On the basis of the correlation coefficient values r^2, the Higuchi model (the r^2 value was 0.9933) turned out to be the most suitable model to describe the DTX release from XM-DTX micelles. The simplified Higuchi model can be described by the following equation: $Q = K\ t^{1/2}$, where Q is the cumulative amount of drug released in time t and K is the Higuchi release rate constant. ►**Fig. 6** shows the experimental data plotted as cumulative percentage drug release versus time. The Higuchi mode showed a good correlation with experimental data as given in ►**Table 1**, indicating that DTX release from XM-DTX micelles was mainly diffusion-controlled.

Pharmacokinetics

Pharmacokinetic studies were conducted in SD rats using DTX at a dose of 10 mg/kg, and Taxotere as a control. Plasma concentration–time curves of DTX after administration of XM-DTX micelles (iv) and Taxotere (iv) are shown in ►**Fig. 7**. Our data showed that the content of DTX in plasma samples of rats in the Taxotere group was less than 0.05 μg/mL at 10 hours, and below the detection limit afterward. Interestingly, intravenous XM-DTX micelles displayed prolonged blood circulation profiles in the plasma, and DTX was still detectable after 24 hours of administration. The main pharmacokinetic parameters of DTX were calculated via DAS 2.0 using a noncompartmental model and are presented in ►**Table 2**.

Table 1 Drug cumulative release kinetics results of XM-DTX micelles

Model	Eqn.	r^2
Zero-order	$Q = 1.3545\ t + 29.283$	0.4536
First-order	$\ln (100 - Q) = -0.1488\ t + 4.5661$	0.9762
Higuchi	$Q = 0.0357\ t^{1/2} - 0.1152$	0.9933
Hixson–Crowell	$(100 - Q)^{1/3} = -0.1616\ t + 4.5102$	0.9481
Weibull	$\ln [\ln (100/(100 - Q))] = -0.0611 \ln t + 0.6214$	0.7916

Abbreviation: Q, amount of drug released in time t.

Table 2 *In vivo* pharmacokinetic parameters (plasma) after intravenous administration of XM-DTX micelles and Taxotere to rats (mean ± SD, $n = 6$)

Parameter	Taxotere	XM-DTX micelles
C_{max} (μg/mL)	4.99 ± 0.24	5.85 ± 0.31
$t_{1/2}$ (h)	2.99 ± 0.35	3.25 ± 0.25
AUC_{0-t} (mg/L × h)	2.56 ± 0.17	6.14 ± 0.36^a
MRT_{0-t} (h)	1.72 ± 0.40	4.70 ± 0.26^a
CL (L/h/kg)	2.998 ± 0.16	1.522 ± 0.24^a

Abbreviations: AUC, area under the plasma concentration–time curve; CL, clearance; C_{max}, peak plasma drug concentration; $t_{1/2}$, elimination half-life; MRT, mean residence time.
[a]$p < 0.05$, versus Taxotere.

Notably, the half-life ($t_{1/2}$) of XM-DTX micelles was 3.25 ± 0.25 hours, as compared with 2.99 ± 0.35 hours for Taxotere, suggesting a longer half-life of the micelles. The maximal plasma concentrations (C_{max}) of XM-DTX micelles and Taxotere were 5.85 ± 0.31 and 4.99 ± 0.24 μg/mL, respectively. XM-DTX micelles have a significantly increased area under the curve by 2.4-fold as compared with Taxotere ($p < 0.05$). The systemic CL of XM-DTX micelles was significantly slower than that of the Taxotere group ($p < 0.05$), which may be attributed to the less removal of XM-DTX micelles through the RES. Differences in CL also led to the observed differences in blood half-life and mean residence time (MRT). Compared with Taxotere, XM-DTX micelles prolonged the MRT of DTX by 2.7-fold. The long circulation time of XM-DTX micelles in the blood can be attributed to their suitable particle size, high negative charge, and hydrophilic surface. Due to misunderstandings about the mechanism of micellar solubilization, micelles are sometimes regarded as the "solution" of the solutes, but this is not the case.[31] Hence, XM-DTX micelles can exhibit different pharmacokinetic performances when compared with intravenous injection solutions. In general, due to the hydrophilic shell, micelles can signal the recognition of the RES, thus, decreasing the CL ratio of RES and leading to a prolonged circulation *in vivo*.[32,33]

Conclusion

DTX is among the most frequently prescribed chemotherapy drugs. However, its poor water solubility prevents the full exploitation of the drug. In this work, we successfully synthesized and evaluated an amphiphilic surfactant, XMeNa, as carrier materials for the delivery of anticancer drugs. Based on XMeNa, XM-DTX micelles were successfully obtained by a sample thin-film hydration method, which allowed an efficient encapsulation of DTX with high EE and DLE. XM-DTX micelles were spherical in morphology with a particle size around 20 nm, and exhibited sustained release property. XM-DTX micelles also prolonged DTX retention in blood circulation, and significantly increased AUC when compared with Taxotere *in vivo*. Given above, XM-DTX micelles have great potential in DTX delivery in cancer therapy. Inspiringly, the amphiphilic surfactant XMeNa could be served as an ideal vehicle for exploring a novel delivery system of poorly water soluble drugs in the future. Although our pharmacokinetic results are quite encouraging, additional studies will be needed to take this potential delivery system to the next level of drug development.

Conflicts of Interest

The authors declared that there are no conflicts of interest.

References

1 Ganju A, Yallapu MM, Khan S, Behrman SW, Chauhan SC, Jaggi M. Nanoways to overcome docetaxel resistance in prostate cancer. Drug Resist Updat 2014;17(1–2):13–23
2 Martin M, Pienkowski T, Mackey J, et al. Breast Cancer International Research Group 001 Investigators. Adjuvant docetaxel for node-positive breast cancer. N Engl J Med 2005;352(22):2302–2313
3 A. Razak SA, Mohd Gazzali A, Fisol FA, et al. Advances in nanocarriers for effective delivery of docetaxel in the treatment of lung cancer: an overview. Cancers (Basel) 2021;13(03):400
4 Imran M, Saleem S, Chaudhuri A, et al. Docetaxel: an update on its molecular mechanisms, therapeutic trajectory and nanotechnology in the treatment of breast, lung and prostate cancer. J Drug Deliv Sci Technol 2020;60:101959
5 Sohail MF, Rehman M, Sarwar HS, et al. Advancements in the oral delivery of Docetaxel: challenges, current state-of-the-art and future trends. Int J Nanomedicine 2018;13:3145–3161
6 Engels FK, Mathot RA, Verweij J. Alternative drug formulations of docetaxel: a review. Anticancer Drugs 2007;18(02):95–103
7 Schwartzberg LS, Navari RM. Safety of polysorbate 80 in the oncology setting. Adv Ther 2018;35(06):754–767
8 Zhang L, Zhang N. How nanotechnology can enhance docetaxel therapy. Int J Nanomedicine 2013;8:2927–2941
9 Ghamkhari A, Pouyafar A, Salehi R, Rahbarghazi R. Chrysin and docetaxel loaded biodegradable micelle for combination chemotherapy of cancer stem cell. Pharm Res 2019;36(12):165
10 Lee SW, Yun MH, Jeong SW, et al. Development of docetaxel-loaded intravenous formulation, Nanoxel-PM™ using polymer-based delivery system. J Control Release 2011;155(02):262–271
11 Hu Q, Rijcken CJ, Bansal R, Hennink WE, Storm G, Prakash J. Complete regression of breast tumour with a single dose of docetaxel-entrapped core-cross-linked polymeric micelles. Biomaterials 2015;53:370–378
12 Atrafi F, Dumez H, Mathijssen RHJ, et al. A phase I dose-escalation and pharmacokinetic study of a micellar nanoparticle with entrapped docetaxel (CPC634) in patients with advanced solid tumours. J Control Release 2020;325:191–197
13 Zhang Y, Huang Y, Li S. Polymeric micelles: nanocarriers for cancer-targeted drug delivery. AAPS PharmSciTech 2014;15 (04):862–871
14 Lu Y, Zhang E, Yang J, Cao Z. Strategies to improve micelle stability for drug delivery. Nano Res 2018;11(10):4985–4998
15 Cheng M, Liu QM, Liu W, et al. Engineering micelles for the treatment and diagnosis of atherosclerosis. J Drug Deliv Sci Technol 2021;63:102473
16 Zheng X, Xie JZ, Zhang X, et al. An overview of polymeric nanomicelles in clinical trials and on the market. Chin Chem Lett 2021; 32:243–257
17 European Medicines Agency. Assessment report for Apealea, EMA/CHMP/785964/2018. 2018;1–121. Accessed February 25, 2022 at: https://www.ema.europa.eu/en/documents/assessment-report/apealea-epar-public-assessment-report_en.pdf.
18 Vergote I, Bergfeldt K, Franquet A, et al. A randomized phase III trial in patients with recurrent platinum sensitive ovarian cancer

comparing efficacy and safety of paclitaxel micellar and Cremophor EL-paclitaxel. Gynecol Oncol 2020;156(02):293–300
19 Borgå O, Lilienberg E, Bjermo H, Hansson F, Heldring N, Dediu R. Pharmacokinetics of total and unbound paclitaxel after administration of paclitaxel micellar or nab-paclitaxel: an open, randomized, cross-over, explorative study in breast cancer patients. Adv Ther 2019;36(10):2825–2837
20 Strelchenok O, Aleksov J. Retinol derivatives, their use in the treatment of cancer and for potentiating the efficacy of other cytotoxic agents. WO Patent 2002SE02087. November, 2002
21 He J, Cheng JJ, Wang ZF, et al. Preparation method of sodium salt of N-(all trans-retinol)-L-cystathionine methyl ester. CN Patent 110218168A. September, 2019
22 Aguiar J, Carpena P, Molina-Bolívar JA, et al. On the determination of the critical micelle concentration by the pyrene 1:3 ratio method. J Colloid Interface Sci 2003;258:116–122
23 Fu PP, Cheng SH, Coop L, et al. Photoreaction, phototoxicity, and photocarcinogenicity of retinoids. J Environ Sci Health Part C Environ Carcinog Ecotoxicol Rev 2003;21(02):165–197
24 Kore G, Kolate A, Nej A, Misra A. Polymeric micelle as multifunctional pharmaceutical carriers. J Nanosci Nanotechnol 2014;14 (01):288–307
25 Torchilin V. Tumor delivery of macromolecular drugs based on the EPR effect. Adv Drug Deliv Rev 2011;63(03):131–135
26 Patil S, Sandberg A, Heckert E, Self W, Seal S. Protein adsorption and cellular uptake of cerium oxide nanoparticles as a function of zeta potential. Biomaterials 2007;28(31):4600–4607
27 Alexis F, Pridgen E, Molnar LK, Farokhzad OC. Factors affecting the clearance and biodistribution of polymeric nanoparticles. Mol Pharm 2008;5(04):505–515
28 Abouelmagd SA, Sun B, Chang AC, Ku YJ, Yeo Y. Release kinetics study of poorly water-soluble drugs from nanoparticles: are we doing it right? Mol Pharm 2015;12(03):997–1003
29 Lee JH, Yeo Y. Controlled drug release from pharmaceutical nanocarriers. Chem Eng Sci 2015;125:75–84
30 Kang M, Lee B, Leal C. Three-dimensional microphase separation and synergistic permeability in stacked lipid-polymer hybrid membranes. Chem Mater 2017;29(21):9120–9132
31 Zoya I, He HS, Wang LT, et al. The intragastrointestinal fate of paclitaxel-loaded micelles: implications on oral drug delivery. Chin Chem Lett 2021;32:1545–1549
32 Zhao J, Chai YD, Zhang J, Huang PF, Nakashima K, Gong YK. Long circulating micelles of an amphiphilic random copolymer bearing cell outer membrane phosphorylcholine zwitterions. Acta Biomater 2015;16:94–102
33 Zheng P, Liu Y, Chen JJ, et al. Targeted pH-responsive polyion complex micelle for controlled intracellular drug delivery. Chin Chem Lett 2020;31:1178–1182